

Estimating AutoAntibody Signatures to Detect Autoimmune Disease Patient Subsets

Zhenke Wu

Assistant Professor
Department of Biostatistics, University of Michigan

27 July 2017



The 62nd Annual International Biometric Society Meeting of the
Brazilian Region (RBras 2017)

R package: [spotgear](#)

<https://github.com/zhenkewu/spotgear>

Common Questions on Individual and Population Health



1.
 - a. What is the person's health state given health measurements?
 - b. What is the population distribution of health states?
(Wu et al., 2015, *JRSS-C*; Wu and Zeger, 2016a,b)
2.
 - a. What is the person's health trajectory?
 - b. What is the population's characteristics of health trajectory?
3. Does a particular intervention improve health - on average/for a particular person? (Wu et al., 2014, *Biometrics*; Frangakis, Qian, Wu, Diaz, 2015, *Biometrics*)
4. Are interventions being used optimally?

Example I

Pneumonia Etiology Research for Child Health (PERCH)

Background:

- > 30 possible infectious causes
- Difficult to directly observe

Goal:

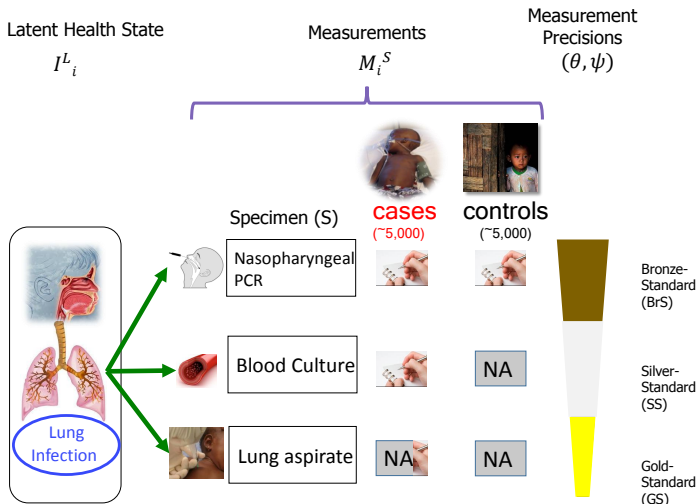
- Population disease etiology estimation
- Individual diagnosis

Study details:

- \$40-mil, Gates-funded 7-country study;
Sites at Sub-Saharan Africa and South Asia
- Diverse measures; variable precisions
- ~5,000 cases and ~5,000 controls



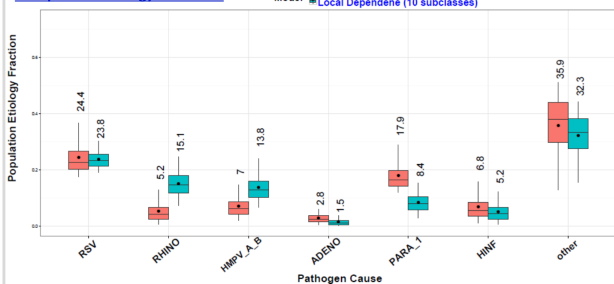
Measurements of Different Quality



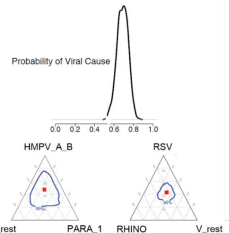
*NP: nasopharyngeal; PCR: polymerase chain reaction; LA: lung aspirate

Nested Partially-Latent Class Models for Population and Individual Estimations

A. Population Etiology Estimation

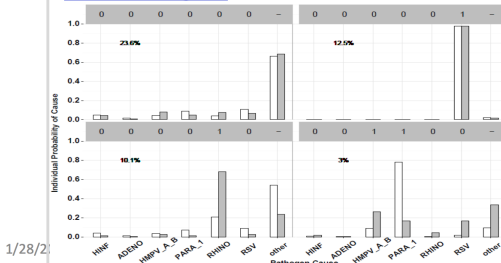


B. Estimation by Pathogen Taxonomy



Marginal posterior distributions of the population etiology for 6 leading pathogens plus other.
Results based on two models are shown.

C. Individual Diagnosis

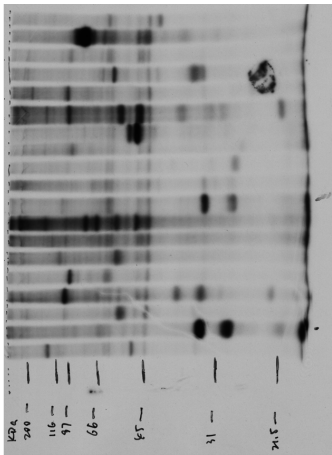


Individual predictions of the cause of pneumonia for 4 patterns of NPPCR data (binary codes in gray bands with its observed frequency shown below). Results from two models are shown. The top two have similar predictions; The bottom two differ, depending on how we correct for false positives.

Example II: Raw Data

Gel Electrophoresis Autoradiography; 20 Samples

Raw Image

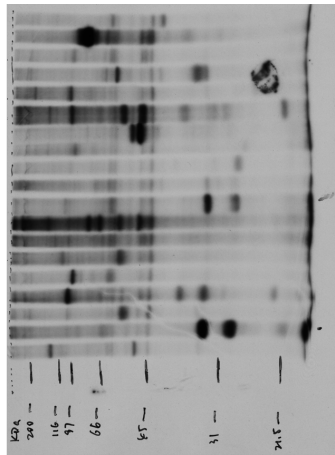


Reference: 1 →

Example II: Raw Data

Gel Electrophoresis Autoradiography; 20 Samples

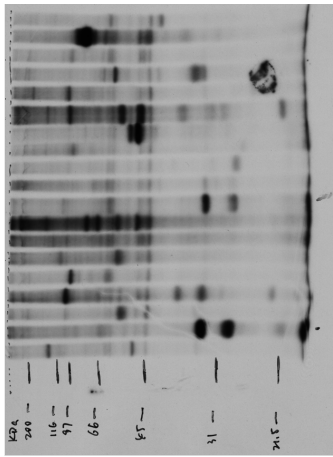
Raw Image



Example II: Raw Data

Gel Electrophoresis Autoradiography; 20 Samples

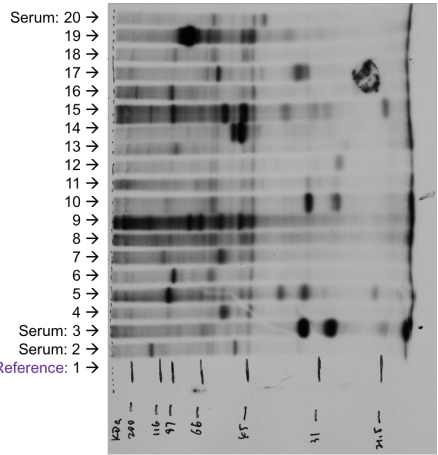
Raw Image



Example II: Raw Data

Gel Electrophoresis Autoradiography; 20 Samples

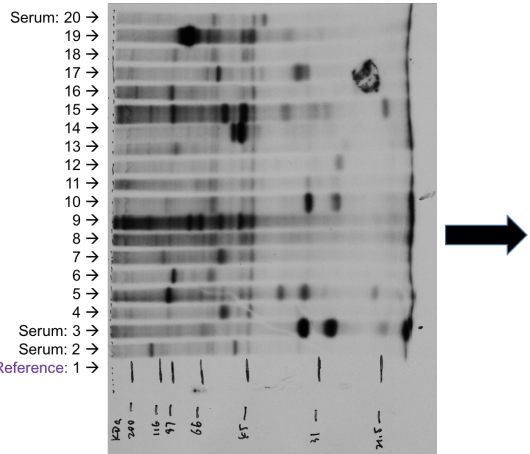
Raw Image



Example II: Raw Data

Gel Electrophoresis Autoradiography; 20 Samples

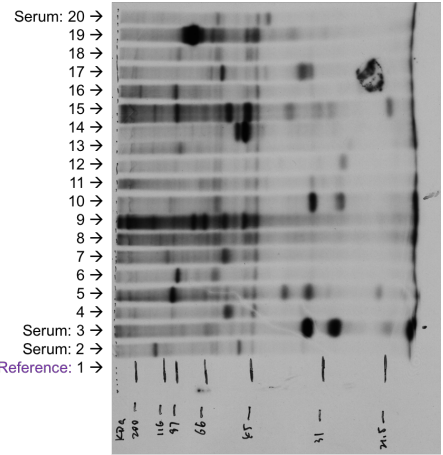
Raw Image



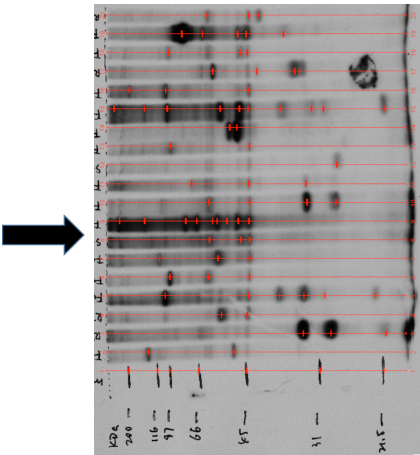
Example II: Raw Data

Gel Electrophoresis Autoradiography; 20 Samples

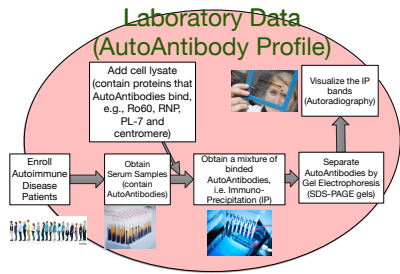
Raw Image



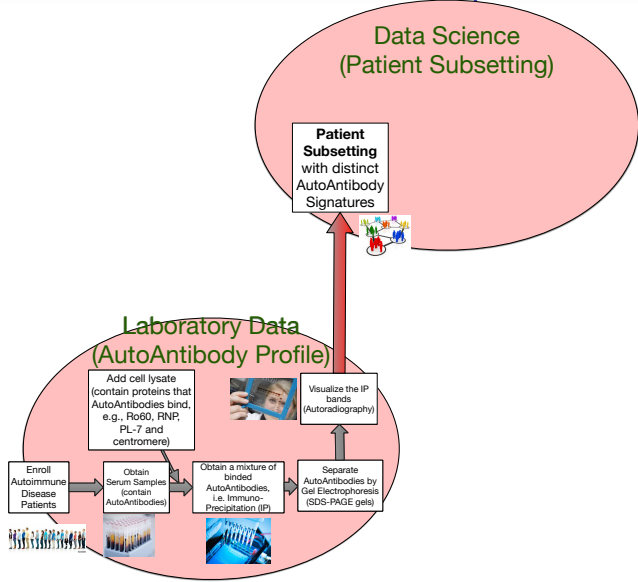
Hand-picked Bands "||"



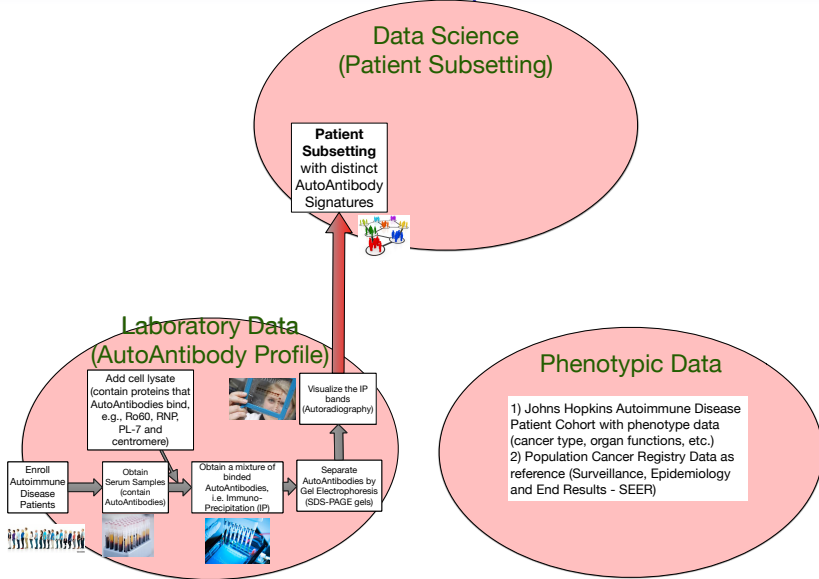
Roadmap



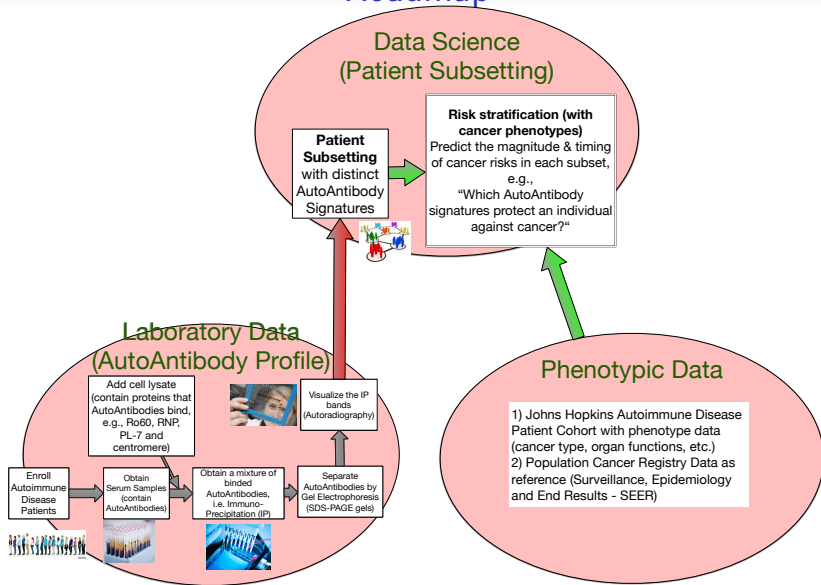
Roadmap



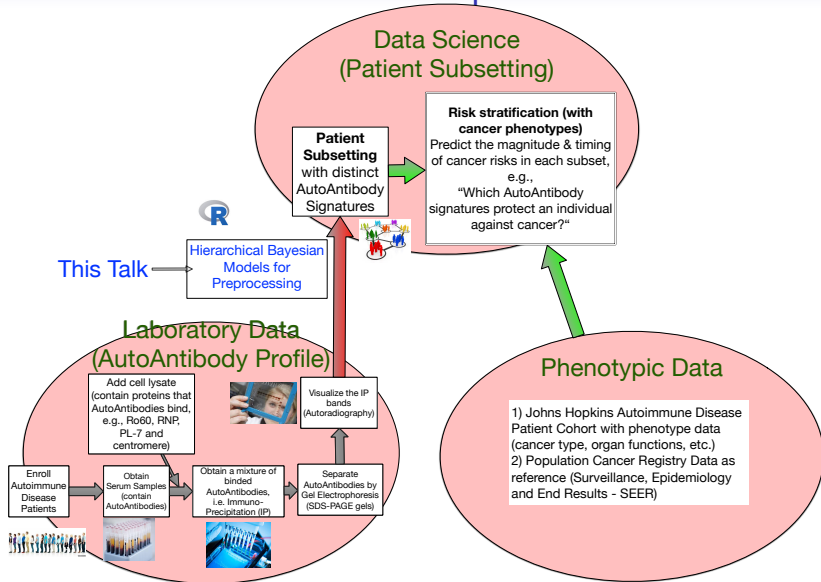
Roadmap



Roadmap



Roadmap



Autoimmune Diseases and AutoAntibody Signatures

- Etiology of Autoimmune Diseases:

Autoimmune Diseases and AutoAntibody Signatures

- Etiology of Autoimmune Diseases:
 - Human immune system's responses to autoantigens;

Autoimmune Diseases and AutoAntibody Signatures

- **Etiology of Autoimmune Diseases:**

- Human immune system's responses to autoantigens;
- The body produces specific autoantibodies that target these autoantigens but also cause tissue damage

Autoimmune Diseases and AutoAntibody Signatures

- **Etiology of Autoimmune Diseases:**
 - Human immune system's responses to autoantigens;
 - The body produces specific autoantibodies that target these autoantigens but also cause tissue damage
- **Heterogeneity:** The autoantibody composition is strikingly different among patients

Autoimmune Diseases and AutoAntibody Signatures

- **Etiology of Autoimmune Diseases:**
 - Human immune system's responses to autoantigens;
 - The body produces specific autoantibodies that target these autoantigens but also cause tissue damage
- **Heterogeneity:** The autoantibody composition is strikingly different among patients
- **Long-term clinical objective:** find autoantibody signature that subsets autoimmune disease patients into groups with more homogeneous phenotypes and trajectories

Autoimmune Diseases and AutoAntibody Signatures

- **Etiology of Autoimmune Diseases:**
 - Human immune system's responses to autoantigens;
 - The body produces specific autoantibodies that target these autoantigens but also cause tissue damage
- **Heterogeneity:** The autoantibody composition is strikingly different among patients
- **Long-term clinical objective:** find autoantibody signature that subsets autoimmune disease patients into groups with more homogeneous phenotypes and trajectories
- **Measurements:**

Autoimmune Diseases and AutoAntibody Signatures

- **Etiology of Autoimmune Diseases:**
 - Human immune system's responses to autoantigens;
 - The body produces specific autoantibodies that target these autoantigens but also cause tissue damage
- **Heterogeneity:** The autoantibody composition is strikingly different among patients
- **Long-term clinical objective:** find autoantibody signature that subsets autoimmune disease patients into groups with more homogeneous phenotypes and trajectories
- **Measurements:** Gel Electrophoresis Autoradiography (GEA)

Gel Electrophoresis Autoradiography (GEA)

A technique to visualize the abundance of molecules or fragments of molecules that have been radioactively labeled.

- Can generate 100s of possibilities of band patterns

Gel Electrophoresis Autoradiography (GEA)

A technique to visualize the abundance of molecules or fragments of molecules that have been radioactively labeled.

- Can generate 100s of possibilities of band patterns
- Can be tested and validated using commercially available line immunoblot assay (EuroImmun; Systemic Sclerosis (Nucleoli) profile)

Gel Electrophoresis Autoradiography (GEA)

A technique to visualize the abundance of molecules or fragments of molecules that have been radioactively labeled.

- Can generate 100s of possibilities of band patterns
- Can be tested and validated using commercially available line immunoblot assay (Euroimmun; Systemic Sclerosis (Nucleoli) profile)
- **Gap:** Onerous and expensive to validate; Need a method to greatly simplify autoantibody profile discovery

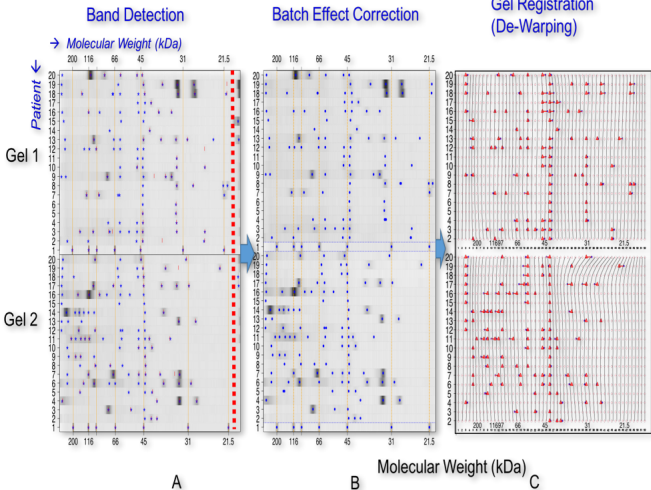
Gel Electrophoresis Autoradiography (GEA)

A technique to visualize the abundance of molecules or fragments of molecules that have been radioactively labeled.

- Can generate 100s of possibilities of band patterns
- Can be tested and validated using commercially available line immunoblot assay (Euroimmun; Systemic Sclerosis (Nucleoli) profile)
- **Gap:** Onerous and expensive to validate; Need a method to greatly simplify autoantibody profile discovery
- **Solution:** Pre-filtering to define subgroups with similar specificities based on the bands observed by GEA

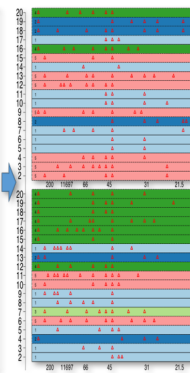
Automated Pipeline for Autoimmune Disease Subsetting

Step I. Pre-Processing IP Data

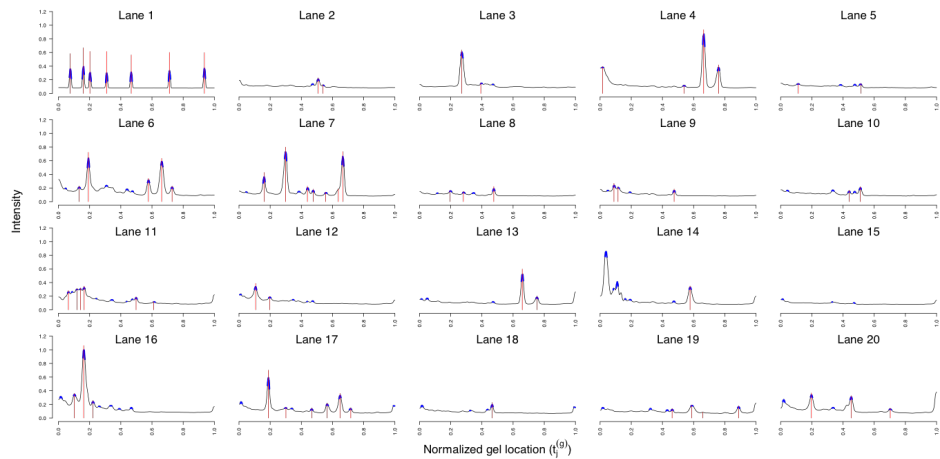


Step II. Discovery of Antibody Subsets

Sera Subgrouping

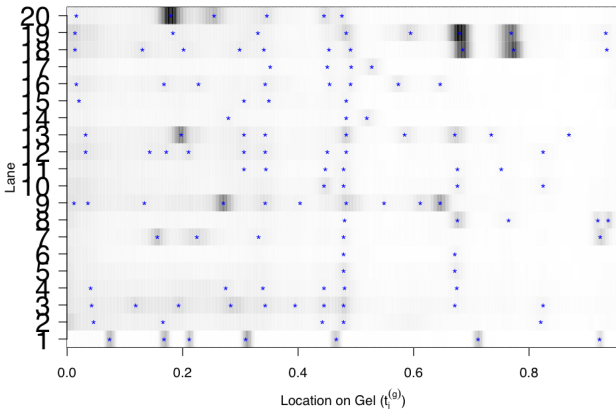


Step I-A: Automated Peak Detection



Step I-A: Automated Peak Detection

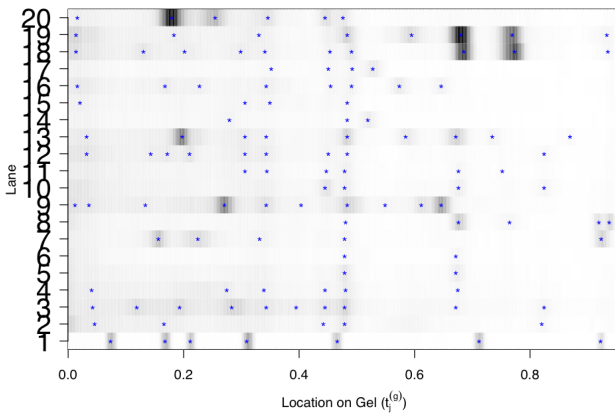
Overlaid against gel image; "*" for detected peaks



- u_{gi} : lane number for lane $i = 1, \dots, N_g$, gel $g = 1, \dots, G$

Step I-A: Automated Peak Detection

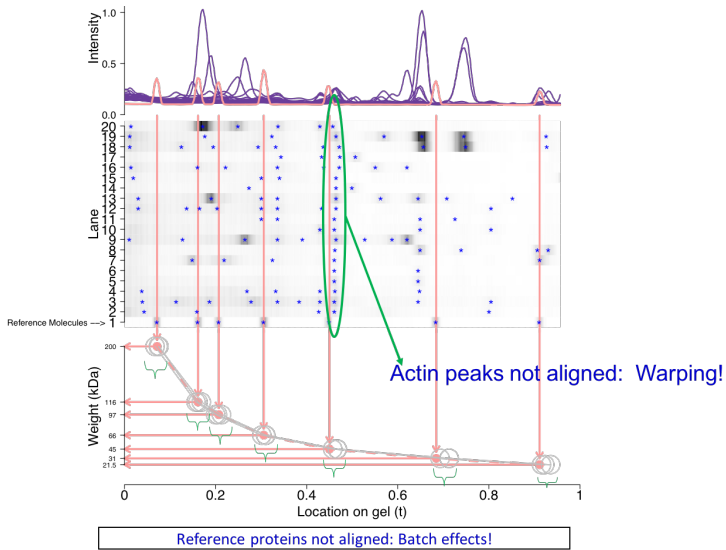
Overlaid against gel image; "*" for detected peaks



- u_{gi} : lane number for lane $i = 1, \dots, N_g$, gel $g = 1, \dots, G$
- T_{gij} : location for the j -th peak ("*"), $j = 1, \dots, J_{gi}$, for lane i , gel g

Step I-B: Batch Effect Correction

Must address before meaningful subgrouping

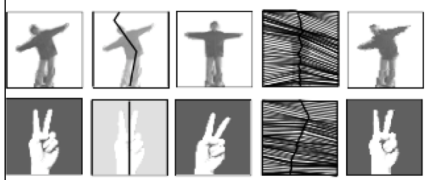


Warping Examples

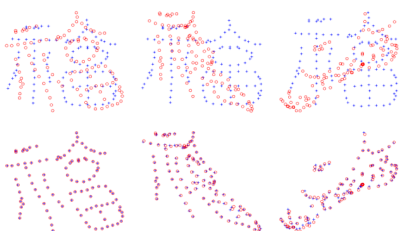
Euclidean Distance: 158.337

Euclidean Distance: 154.0287

Euclidean Distance: 515.7095



Motion Alignment: Uchida and Sakoe,

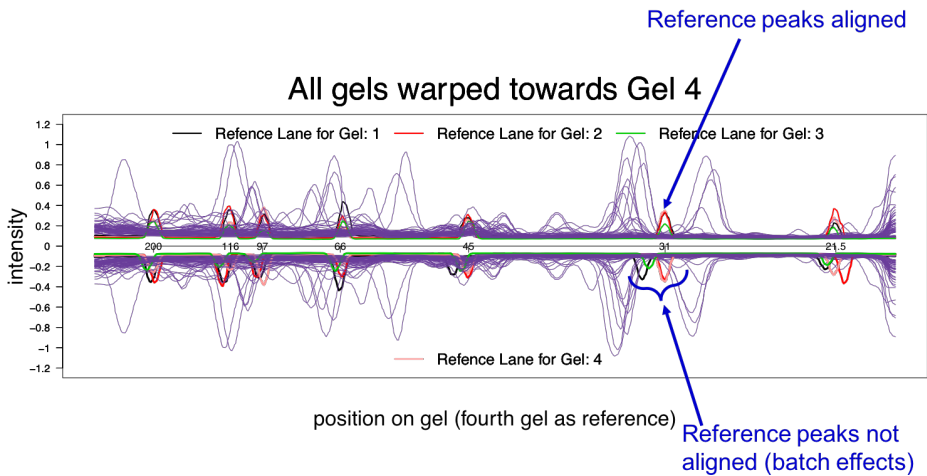


Signature Verification: Hastie et al. 1991

Handwritten Chinese: Ma and Zhao
(2015)

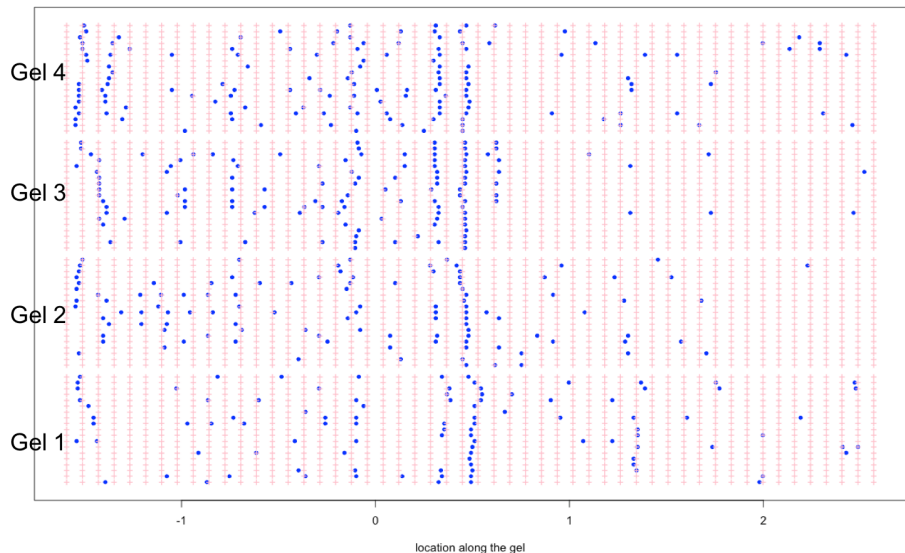
Step I-B: Batch Effect Correction

Piecewise Linear Warping by Reference Marker Molecules



Step I-C: Align the peaks

"Which "+" do the peaks "●" belong?"



Step I-C: Two-Dimensional De-Warping

- The physical process of autoradiography could cause image deformation
- Challenges
 - In general, few light-weight proteins on the right side of the image; If we don't see bands, how to align?
Solution: align to a grid of protein landmarks and assume smoothness of warping

Step I-C: Two-Dimensional De-Warping

- The physical process of autoradiography could cause image deformation
- Challenges
 - In general, few light-weight proteins on the right side of the image; If we don't see bands, how to align?
Solution: align to a grid of protein landmarks and assume smoothness of warping
 - Ubiquitous proteins (e.g., actin) on multiple gels must be aligned.
Solution: Discretized non-homogeneous Poisson process with shared intensity across gels

Step I-C: Two-Dimensional De-Warping

- The physical process of autoradiography could cause image deformation
- Challenges
 - In general, few light-weight proteins on the right side of the image; If we don't see bands, how to align?
Solution: align to a grid of protein landmarks and assume smoothness of warping
 - Ubiquitous proteins (e.g., actin) on multiple gels must be aligned.
Solution: Discretized non-homogeneous Poisson process with shared intensity across gels
 - The observed peak locations are noisy.
Solution: Gaussian noise around the true location

Step I-C: Model for 2-Dimensional Image Dewarping

Prior on the peak-to-landmark indicators

- Peak-to-landmark Indicators:

Step I-C: Model for 2-Dimensional Image Dewarping

Prior on the peak-to-landmark indicators

- Peak-to-landmark Indicators:

1. $Z_{gij} \in \{1, \dots, L\}$, $j = 1, \dots, J_{gi}$ (match a “*” to a “+”), e.g., $Z_{gij} = 3$ means the peak is matched to Landmark 3

Step I-C: Model for 2-Dimensional Image Dewarping

Prior on the peak-to-landmark indicators

- Peak-to-landmark Indicators:

1. $Z_{gij} \in \{1, \dots, L\}$, $j = 1, \dots, J_{gi}$ (match a “ $*$ ” to a “ $+$ ”), e.g., $Z_{gij} = 3$ means the peak is matched to Landmark 3
2. Constrain $Z_{gi,j-1} \leq Z_{gij}$ to prevent reverse matching

Step I-C: Model for 2-Dimensional Image Dewarping

Prior on the peak-to-landmark indicators

- Peak-to-landmark Indicators:
 1. $Z_{gij} \in \{1, \dots, L\}$, $j = 1, \dots, J_{gi}$ (match a “ $*$ ” to a “ $+$ ”), e.g., $Z_{gij} = 3$ means the peak is matched to Landmark 3
 2. Constrain $Z_{gi,j-1} \leq Z_{gij}$ to prevent reverse matching
- Bayesian Model for Aligning Peaks to Landmarks

Step I-C: Model for 2-Dimensional Image Dewarping

Prior on the peak-to-landmark indicators

- Peak-to-landmark Indicators:
 1. $Z_{gij} \in \{1, \dots, L\}$, $j = 1, \dots, J_{gi}$ (match a “ $*$ ” to a “ $+$ ”), e.g., $Z_{gij} = 3$ means the peak is matched to Landmark 3
 2. Constrain $Z_{gi,j-1} \leq Z_{gij}$ to prevent reverse matching
- Bayesian Model for Aligning Peaks to Landmarks
 - Number of observed peaks in lane i , gel g :
$$J_{gi} \stackrel{d}{\sim} \text{Poisson}(\Lambda)$$

Step I-C: Model for 2-Dimensional Image Dewarping

Prior on the peak-to-landmark indicators

- Peak-to-landmark Indicators:
 1. $Z_{gij} \in \{1, \dots, L\}$, $j = 1, \dots, J_{gi}$ (match a “*” to a “+”), e.g.,
 $Z_{gij} = 3$ means the peak is matched to Landmark 3
 2. Constrain $Z_{gi,j-1} \leq Z_{gij}$ to prevent reverse matching
- Bayesian Model for Aligning Peaks to Landmarks
 - Number of observed peaks in lane i , gel g :
 $J_{gi} \stackrel{d}{\sim} \text{Poisson}(\Lambda)$
 Λ : Cumulative intensity; Controls the total number of peaks

Step I-C: Model for 2-Dimensional Image Dewarping

Prior on the peak-to-landmark indicators

- Peak-to-landmark Indicators:
 1. $Z_{gij} \in \{1, \dots, L\}$, $j = 1, \dots, J_{gi}$ (match a “ $*$ ” to a “ $+$ ”), e.g., $Z_{gij} = 3$ means the peak is matched to Landmark 3
 2. Constrain $Z_{gi,j-1} \leq Z_{gij}$ to prevent reverse matching
- Bayesian Model for Aligning Peaks to Landmarks
 - Number of observed peaks in lane i , gel g :
 $J_{gi} \stackrel{d}{\sim} \text{Poisson}(\Lambda)$
 Λ : Cumulative intensity; Controls the total number of peaks
 - Peak-to-landmark indicators:
 $(Z_{g i 1}, \dots, Z_{g i J_{g i}}) = \text{increasing sort } \{Z_{g i 1}^*, \dots, Z_{g i J_{g i}}^*\}$

Step I-C: Model for 2-Dimensional Image Dewarping

Prior on the peak-to-landmark indicators

- Peak-to-landmark Indicators:
 1. $Z_{gij} \in \{1, \dots, L\}$, $j = 1, \dots, J_{gi}$ (match a “ $*$ ” to a “ $+$ ”), e.g., $Z_{gij} = 3$ means the peak is matched to Landmark 3
 2. Constrain $Z_{gi,j-1} \leq Z_{gij}$ to prevent reverse matching
- Bayesian Model for Aligning Peaks to Landmarks
 - Number of observed peaks in lane i , gel g :
 $J_{gi} \stackrel{d}{\sim} \text{Poisson}(\Lambda)$
 Λ : Cumulative intensity; Controls the total number of peaks
 - Peak-to-landmark indicators:
 $(Z_{gi1}, \dots, Z_{giJ_{gi}}) = \text{increasing sort } \{Z_{gi1}^*, \dots, Z_{giJ_{gi}}^*\}$
 - $Z_{gij}^* \stackrel{iid}{\sim} \text{Categorical} \left(\{\lambda_\ell^*\}_{\ell=1}^L \right)$

Step I-C: Model for 2-Dimensional Image Dewarping

Prior on the peak-to-landmark indicators

- Peak-to-landmark Indicators:
 1. $Z_{gij} \in \{1, \dots, L\}$, $j = 1, \dots, J_{gi}$ (match a “*” to a “+”), e.g., $Z_{gij} = 3$ means the peak is matched to Landmark 3
 2. Constrain $Z_{gi,j-1} \leq Z_{gij}$ to prevent reverse matching
- Bayesian Model for Aligning Peaks to Landmarks
 - Number of observed peaks in lane i , gel g :
 $J_{gi} \stackrel{d}{\sim} \text{Poisson}(\Lambda)$
 Λ : Cumulative intensity; Controls the total number of peaks
 - Peak-to-landmark indicators:
 $(Z_{gi1}, \dots, Z_{giJ_{gi}}) = \text{increasing sort } \{Z_{gi1}^*, \dots, Z_{giJ_{gi}}^*\}$
 - $Z_{gij}^* \stackrel{iid}{\sim} \text{Categorical} \left(\{\lambda_\ell^*\}_{\ell=1}^L \right)$
 λ_ℓ^* : Landmark-specific intensity; Independent of g ; Hence, when possible, encourages nearby peaks to be aligned to an identical landmark

Step I-C: 2-Dimensional Image Dewarping

Gaussian Mixture Model for Noisy Peak Locations “*”

- Model the observed peaks T_{gij} as observations from a L -component Gaussian mixture, for each candidate landmark ℓ

Step I-C: 2-Dimensional Image Dewarping

Gaussian Mixture Model for Noisy Peak Locations “*”

- Model the observed peaks T_{gij} as observations from a L -component Gaussian mixture, for each candidate landmark ℓ
- We assume

$$p \left\{ \underbrace{(T_{gij} = t, u_{gi})}_{\text{peak location}}, \underbrace{u_{gi}}_{\text{lane number}} \mid \underbrace{Z_{gij} = \ell}_{\text{matched to landmark } \ell}, \underbrace{T_{gi,j-1}}_{\text{nearest left peak location}}, \underbrace{\mathcal{S}_g}_{\text{warping function}}, \underbrace{\sigma_\epsilon}_{\text{noise level}} \right\}$$

$$= \begin{cases} \phi(t; \mathcal{S}_g(\nu_\ell, u_{gi}), \sigma_\epsilon), & t \in \mathcal{I}_{gij}(\nu_\ell, A_0); \\ 0, & \text{otherwise,} \end{cases}$$

$\ell = 1, \dots, L$, peak $j = 1, \dots, J_{gi}$, lane $i = 1, \dots, N_g$, gel $g = 1, \dots, G$.

Step I-C: 2-Dimensional Image Dewarping

Gaussian Mixture Model for Noisy Peak Locations “*”

- Model the observed peaks T_{gij} as observations from a L -component Gaussian mixture, for each candidate landmark ℓ
- We assume

$$p \left\{ \underbrace{(T_{gij} = t, u_{gi})}_{\text{peak location}}, \underbrace{u_{gi}}_{\text{lane number}} \mid \underbrace{Z_{gij} = \ell}_{\substack{\text{matched to} \\ \text{landmark } \ell}}, \underbrace{T_{gi,j-1}}_{\substack{\text{nearest left} \\ \text{peak location}}}, \underbrace{\mathcal{S}_g}_{\substack{\text{warping} \\ \text{function}}}, \underbrace{\sigma_\epsilon}_{\text{noise level}} \right\}$$

$$= \begin{cases} \phi(t; \mathcal{S}_g(\nu_\ell, u_{gi}), \sigma_\epsilon), & t \in \mathcal{I}_{gij}(\nu_\ell, A_0); \\ 0, & \text{otherwise,} \end{cases}$$

$$\ell = 1, \dots, L, \text{ peak } j = 1, \dots, J_{gi}, \text{ lane } i = 1, \dots, N_g, \text{ gel } g = 1, \dots, G.$$

- $\phi(\cdot; a, b)$: Gaussian density with mean a and standard deviation b .

Step I-C: 2-Dimensional Image Dewarping

Gaussian Mixture Model for Noisy Peak Locations “*”

- Model the observed peaks T_{gij} as observations from a L -component Gaussian mixture, for each candidate landmark ℓ
- We assume

$$p \left\{ \underbrace{(T_{gij} = t)}_{\text{peak location}}, \underbrace{u_{gi}}_{\text{lane number}} \mid \underbrace{Z_{gij} = \ell}_{\text{matched to landmark } \ell}, \underbrace{T_{gi,j-1}}_{\text{nearest left peak location}}, \underbrace{\mathcal{S}_g}_{\text{warping function}}, \underbrace{\sigma_\epsilon}_{\text{noise level}} \right\}$$

$$= \begin{cases} \phi(t; \mathcal{S}_g(\nu_\ell, u_{gi}), \sigma_\epsilon), & t \in \mathcal{I}_{gij}(\nu_\ell, A_0); \\ 0, & \text{otherwise,} \end{cases}$$

$\ell = 1, \dots, L$, peak $j = 1, \dots, J_{gi}$, lane $i = 1, \dots, N_g$, gel $g = 1, \dots, G$.

- $\mathcal{S}_g: (\nu_\ell, u_{gi}) \mapsto \mathcal{S}_g(\nu_\ell, u_i)$, *unknown*, smooth bivariate function for the spatial deformation

Step I-C: 2-Dimensional Image Dewarping

Gaussian Mixture Model for Noisy Peak Locations “*”

- Model the observed peaks T_{gij} as observations from a L -component Gaussian mixture, for each candidate landmark ℓ
- We assume

$$p \left\{ \underbrace{(T_{gij} = t)}_{\text{peak location}}, \underbrace{u_{gi}}_{\text{lane number}} \mid \underbrace{Z_{gij} = \ell}_{\substack{\text{matched to} \\ \text{landmark } \ell}}, \underbrace{T_{gi,j-1}}_{\substack{\text{nearest left} \\ \text{peak location}}}, \underbrace{\mathcal{S}_g}_{\substack{\text{warping} \\ \text{function}}}, \underbrace{\sigma_\epsilon}_{\text{noise level}} \right\}$$

$$= \begin{cases} \phi(t; \mathcal{S}_g(\nu_\ell, u_{gi}), \sigma_\epsilon), & t \in \mathcal{I}_{gij}(\nu_\ell, A_0); \\ 0, & \text{otherwise,} \end{cases}$$

$\ell = 1, \dots, L$, peak $j = 1, \dots, J_{gi}$, lane $i = 1, \dots, N_g$, gel $g = 1, \dots, G$.

- The set $\mathcal{I}_{gij}(\nu_\ell, A_0) \triangleq \{t : |t - \nu_\ell| < A_0 \text{ and } t > T_{gi,j-1}\}$ assumes a peak appears within distance A_0 from its true landmark

Step I-C: 2-Dimensional Image Dewarping

Gaussian Mixture Model for Noisy Peak Locations “*”

- Model the observed peaks T_{gij} as observations from a L -component Gaussian mixture, for each candidate landmark ℓ
- We assume

$$p \left\{ \underbrace{(T_{gij} = t, u_{gi})}_{\text{peak location}}, \underbrace{u_{gi}}_{\text{lane number}} \mid \underbrace{Z_{gij} = \ell}_{\substack{\text{matched to} \\ \text{landmark } \ell}}, \underbrace{T_{gi,j-1}}_{\substack{\text{nearest left} \\ \text{peak location}}}, \underbrace{\mathcal{S}_g}_{\substack{\text{warping} \\ \text{function}}}, \underbrace{\sigma_\epsilon}_{\text{noise level}} \right\}$$

$$= \begin{cases} \phi(t; \mathcal{S}_g(\nu_\ell, u_{gi}), \sigma_\epsilon), & t \in \mathcal{I}_{gij}(\nu_\ell, A_0); \\ 0, & \text{otherwise,} \end{cases}$$

$\ell = 1, \dots, L$, peak $j = 1, \dots, J_{gi}$, lane $i = 1, \dots, N_g$, gel $g = 1, \dots, G$.

- Let \mathcal{P}_g be the peaks for gel g ; let \mathcal{P} collect all the peaks

Step I-C: 2-Dimensional Image Dewarping

Warping Function by Tensor Product Basis Expansion

- We assume the warping function

$$\mathcal{S}_g(\nu, u) = \sum_{s=1}^{T_\nu} \sum_{t=1}^{T_u} \beta_{gst} B_{g1s}(\nu) B_{g2t}(u),$$

Step I-C: 2-Dimensional Image Dewarping

Warping Function by Tensor Product Basis Expansion

- We assume the warping function

$$\mathcal{S}_g(\nu, u) = \sum_{s=1}^{T_\nu} \sum_{t=1}^{T_u} \beta_{gst} B_{g1s}(\nu) B_{g2t}(u),$$

- $B_{g1s}(\cdot)$ and $B_{g2t}(\cdot)$: the s -th and t -th cubic B-spline basis along the two coordinate directions, respectively

Step I-C: 2-Dimensional Image Dewarping

Warping Function by Tensor Product Basis Expansion

- We assume the warping function

$$\mathcal{S}_g(\nu, u) = \sum_{s=1}^{T_\nu} \sum_{t=1}^{T_u} \beta_{gst} B_{g1s}(\nu) B_{g2t}(u),$$

- $B_{g1s}(\cdot)$ and $B_{g2t}(\cdot)$: the s -th and t -th cubic B-spline basis along the two coordinate directions, respectively
- $\{\beta_{gst}\}$: the set of coefficients to be estimated

Step I-C: 2-Dimensional Image Dewarping

Warping Function by Tensor Product Basis Expansion

- We assume the warping function

$$\mathcal{S}_g(\nu, u) = \sum_{s=1}^{T_\nu} \sum_{t=1}^{T_u} \beta_{gst} B_{g1s}(\nu) B_{g2t}(u),$$

- $B_{g1s}(\cdot)$ and $B_{g2t}(\cdot)$: the s -th and t -th cubic B-spline basis along the two coordinate directions, respectively
- $\{\beta_{gst}\}$: the set of coefficients to be estimated
- **Implementing Warping Function Constraints and Priors**

Step I-C: 2-Dimensional Image Dewarping

Warping Function by Tensor Product Basis Expansion

- We assume the warping function

$$\mathcal{S}_g(\nu, u) = \sum_{s=1}^{T_\nu} \sum_{t=1}^{T_u} \beta_{gst} B_{g1s}(\nu) B_{g2t}(u),$$

- $B_{g1s}(\cdot)$ and $B_{g2t}(\cdot)$: the s -th and t -th cubic B-spline basis along the two coordinate directions, respectively
- $\{\beta_{gst}\}$: the set of coefficients to be estimated
- **Implementing Warping Function Constraints and Priors**
 - Boundary constraint: $\mathcal{S}_g(\nu_0, u) = \nu_0, \mathcal{S}_g(\nu_{L+1}, u) = \nu_{L+1}$

Step I-C: 2-Dimensional Image Dewarping

Warping Function by Tensor Product Basis Expansion

- We assume the warping function

$$\mathcal{S}_g(\nu, u) = \sum_{s=1}^{T_\nu} \sum_{t=1}^{T_u} \beta_{gst} B_{g1s}(\nu) B_{g2t}(u),$$

- $B_{g1s}(\cdot)$ and $B_{g2t}(\cdot)$: the s -th and t -th cubic B-spline basis along the two coordinate directions, respectively
- $\{\beta_{gst}\}$: the set of coefficients to be estimated
- Implementing Warping Function Constraints and Priors**
 - Boundary constraint: $\mathcal{S}_g(\nu_0, u) = \nu_0, \mathcal{S}_g(\nu_{L+1}, u) = \nu_{L+1}$
 - Monotonic constraint:
 $\nu_0 < \mathcal{S}_g(\nu_{\ell-1}, u) < \mathcal{S}_g(\nu_\ell, u) < \nu_{L+1}, \forall \ell = 1, \dots, L, \forall u$

Step I-C: 2-Dimensional Image Dewarping

Warping Function by Tensor Product Basis Expansion

- We assume the warping function

$$\mathcal{S}_g(\nu, u) = \sum_{s=1}^{T_\nu} \sum_{t=1}^{T_u} \beta_{gst} B_{g1s}(\nu) B_{g2t}(u),$$

- $B_{g1s}(\cdot)$ and $B_{g2t}(\cdot)$: the s -th and t -th cubic B-spline basis along the two coordinate directions, respectively
- $\{\beta_{gst}\}$: the set of coefficients to be estimated
- Implementing Warping Function Constraints and Priors**
 - Boundary constraint: $\mathcal{S}_g(\nu_0, u) = \nu_0, \mathcal{S}_g(\nu_{L+1}, u) = \nu_{L+1}$
 - Monotonic constraint:
 $\nu_0 < \mathcal{S}_g(\nu_{\ell-1}, u) < \mathcal{S}_g(\nu_\ell, u) < \nu_{L+1}, \forall \ell = 1, \dots, L, \forall u$
 - Both constraints above can be implemented via constraints on $\{\beta_{gst}\}$**

Step I-C: 2-Dimensional Image Dewarping

Warping Function by Tensor Product Basis Expansion

- We assume the warping function

$$\mathcal{S}_g(\nu, u) = \sum_{s=1}^{T_\nu} \sum_{t=1}^{T_u} \beta_{gst} B_{g1s}(\nu) B_{g2t}(u),$$

- $B_{g1s}(\cdot)$ and $B_{g2t}(\cdot)$: the s -th and t -th cubic B-spline basis along the two coordinate directions, respectively
- $\{\beta_{gst}\}$: the set of coefficients to be estimated
- Implementing Warping Function Constraints and Priors**
 - Boundary constraint: $\mathcal{S}_g(\nu_0, u) = \nu_0, \mathcal{S}_g(\nu_{L+1}, u) = \nu_{L+1}$
 - Monotonic constraint:
 $\nu_0 < \mathcal{S}_g(\nu_{\ell-1}, u) < \mathcal{S}_g(\nu_\ell, u) < \nu_{L+1}, \forall \ell = 1, \dots, L, \forall u$
 - Both constraints above can be implemented via constraints on $\{\beta_{gst}\}$**
 - Smoothness: Bayesian penalized-splines to make adjacent $\{\beta_{gst}\}$ similar

Step I-C: 2-Dimensional Image Dewarping

Warping Function by Tensor Product Basis Expansion

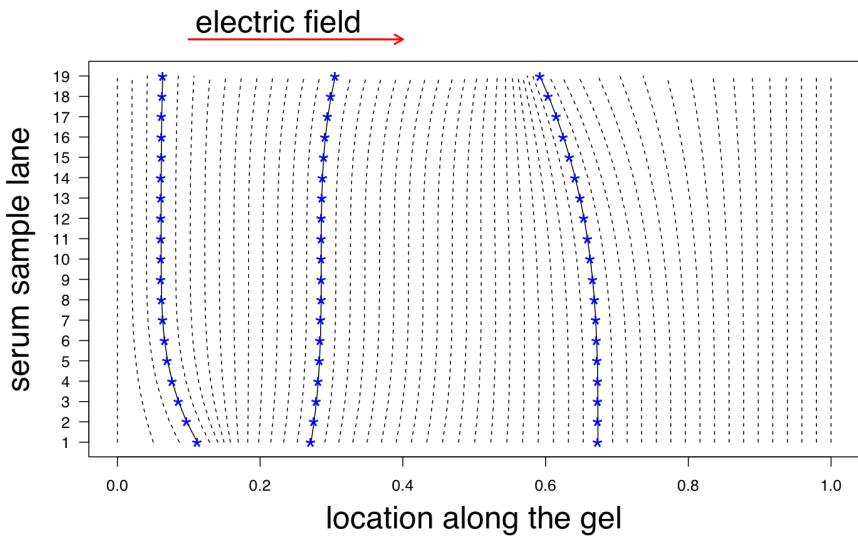
- We assume the warping function

$$\mathcal{S}_g(\nu, u) = \sum_{s=1}^{T_\nu} \sum_{t=1}^{T_u} \beta_{gst} B_{g1s}(\nu) B_{g2t}(u),$$

- $B_{g1s}(\cdot)$ and $B_{g2t}(\cdot)$: the s -th and t -th cubic B-spline basis along the two coordinate directions, respectively
- $\{\beta_{gst}\}$: the set of coefficients to be estimated
- Implementing Warping Function Constraints and Priors**
 - Boundary constraint: $\mathcal{S}_g(\nu_0, u) = \nu_0, \mathcal{S}_g(\nu_{L+1}, u) = \nu_{L+1}$
 - Monotonic constraint:
 $\nu_0 < \mathcal{S}_g(\nu_{\ell-1}, u) < \mathcal{S}_g(\nu_\ell, u) < \nu_{L+1}, \forall \ell = 1, \dots, L, \forall u$
 - Both constraints above can be implemented via constraints on $\{\beta_{gst}\}$**
 - Smoothness: Bayesian penalized-splines to make adjacent $\{\beta_{gst}\}$ similar
 - Vary by gel: $\mathcal{S}_g(\nu_\ell, u)$

Step I-C: A Mathematical Model for Warping

Estimate the warping, then reverse



Step I-C: Goal of 2-Dimensional Image De-warping

The posterior distribution $[Z | \mathcal{P}]$

Recall:

- Z : the collection of peak-to-landmark indicators

Step I-C: Goal of 2-Dimensional Image De-warping

The posterior distribution $[Z | \mathcal{P}]$

Recall:

- Z : the collection of peak-to-landmark indicators
- \mathcal{P} : the collection of all the observed peaks

Step I-C: Posterior Inference of the De-Warping

Joint distribution $[\mathcal{P}, \mathbf{Z}]$:

$$\begin{aligned}
 & \prod_{g=1}^G \left\{ \underbrace{\prod_{i=1}^{N_g} \left[\prod_{j=1}^{J_{gi}} N(T_{gij}; \mathbf{B}_{g1}(\nu_{Z_{gij}})' \boldsymbol{\beta}_g \mathbf{B}_{g2}(u_{gi}), \sigma_\epsilon^{-2}) \mathbf{1}\{T_{gij} \in \mathcal{I}_{gij}(\nu_{Z_{gij}}, A_0)\}} \right]}_{\text{likelihood (2.2)}} \right. \\
 & \times J_{gi}! \underbrace{\prod_{j=1}^{J_{gi}} \text{Categorical}(Z_{gij}; \boldsymbol{\lambda}) \mathbf{1}\{Z_{gij} \leq Z_{gi,j+1}, j = 1, \dots, J_{gi} - 1\}}_{\text{prior of } \mathbf{Z}} \Big] \\
 & \times \underbrace{N_{T_\nu-1} \left(\{\beta_{gs1}\}_{s=1}^{T_\nu-1}; \boldsymbol{\beta}_{[-T_\nu]}^{\text{id}}, \sigma_{g1}^{-2} \Delta_1' \Delta_1 \right) \mathbf{1}\{\nu_0 = \beta_{g11} < \dots < \beta_{gs1} < \dots < \beta_{g,T_\nu-1,1} < \nu_{L+1}\} \cdot p(\sigma_{g1}^2)}_{\text{prior (2.6) and hyperprior of the smoothing parameter}} \\
 & \times \underbrace{\prod_{s=2}^{T_\nu-1} \left[N_{T_u} \left(\{\beta_{gst}\}_{t=1}^{T_u}; \mathbf{0}, \sigma_{gs}^{-2} \Delta_2' \Delta_2 \right) \cdot p(\sigma_{gs}^2, \rho_g) \right] \}_{s=2} \times \underbrace{p(\boldsymbol{\lambda})}_{\text{hyperprior for } \mathbf{Z}}, \tag{2.9}
 \end{aligned}$$

prior (2.7) and hyperpriors of the smoothing parameters

- **Goal:** Joint distribution $[\mathcal{P}, \mathbf{Z}]$ (data+unknowns) → Posterior distribution $[\mathbf{Z} | \mathcal{P}]$ (unknown given data)

Step I-C: Posterior Inference of the De-Warping

Joint distribution $[\mathcal{P}, \mathbf{Z}]$:

$$\begin{aligned}
 & \prod_{g=1}^G \left\{ \underbrace{\prod_{i=1}^{N_g} \left[\prod_{j=1}^{J_{gi}} N(T_{gij}; \mathbf{B}_{g1}(\nu_{Z_{gij}})' \boldsymbol{\beta}_g \mathbf{B}_{g2}(u_{gi}), \sigma_\epsilon^{-2}) \mathbf{1}\{T_{gij} \in \mathcal{I}_{gij}(\nu_{Z_{gij}}, A_0)\}} \right]}_{\text{likelihood (2.2)}} \right. \\
 & \times J_{gi}! \underbrace{\prod_{j=1}^{J_{gi}} \text{Categorical}(Z_{gij}; \boldsymbol{\lambda}) \mathbf{1}\{Z_{gij} \leq Z_{gi,j+1}, j = 1, \dots, J_{gi} - 1\}}_{\text{prior of } \mathbf{Z}} \Big] \\
 & \times \underbrace{N_{T_\nu-1} \left(\{\beta_{gs1}\}_{s=1}^{T_\nu-1}; \boldsymbol{\beta}_{[-T_\nu]}^{\text{id}}, \sigma_{g1}^{-2} \Delta_1' \Delta_1 \right) \mathbf{1}\{\nu_0 = \beta_{g11} < \dots < \beta_{gs1} < \dots < \beta_{g,T_\nu-1,1} < \nu_{L+1}\} \cdot p(\sigma_{g1}^2)}_{\text{prior (2.6) and hyperprior of the smoothing parameter}} \\
 & \times \underbrace{\prod_{s=2}^{T_\nu-1} \left[N_{T_u} \left(\{\beta_{gst}\}_{t=1}^{T_u}; \mathbf{0}, \sigma_{gs}^{-2} \Delta_2' \Delta_2 \right) \cdot p(\sigma_{gs}^2, \rho_g) \right] \}_{s=2} \times \underbrace{p(\boldsymbol{\lambda})}_{\text{hyperprior for } \mathbf{Z}}, \tag{2.9}
 \end{aligned}$$

- **Goal:** Joint distribution $[\mathcal{P}, \mathbf{Z}]$ (data+unknowns) → Posterior distribution $[\mathbf{Z} | \mathcal{P}]$ (unknown given data)
- **Tool:** Markov chain Monte Carlo (MCMC)

Step I-C: Posterior Inference of the De-Warping

Joint distribution $[\mathcal{P}, \mathbf{Z}]$:

$$\begin{aligned}
 & \prod_{g=1}^G \left\{ \underbrace{\prod_{i=1}^{N_g} \left[\prod_{j=1}^{J_{gi}} N(T_{gij}; \mathbf{B}_{g1}(\nu_{Z_{gij}})' \boldsymbol{\beta}_g \mathbf{B}_{g2}(u_{gi}), \sigma_\epsilon^{-2}) \mathbf{1}\{T_{gij} \in \mathcal{I}_{gij}(\nu_{Z_{gij}}, A_0)\} \right]}_{\text{likelihood (2.2)}} \right. \\
 & \times J_{gi}! \underbrace{\prod_{j=1}^{J_{gi}} \text{Categorical}(Z_{gij}; \boldsymbol{\lambda}) \mathbf{1}\{Z_{gij} \leq Z_{gi,j+1}, j = 1, \dots, J_{gi} - 1\}}_{\text{prior of } \mathbf{Z}} \Big] \\
 & \times \underbrace{N_{T_\nu-1} \left(\{\beta_{gs1}\}_{s=1}^{T_\nu-1}; \boldsymbol{\beta}_{[-T_\nu]}^{\text{id}}, \sigma_{g1}^{-2} \Delta_1' \Delta_1 \right) \mathbf{1}\{\nu_0 = \beta_{g11} < \dots < \beta_{gs1} < \dots < \beta_{g,T_\nu-1,1} < \nu_{L+1}\} \cdot p(\sigma_{g1}^2)}_{\text{prior (2.6) and hyperprior of the smoothing parameter}} \\
 & \times \underbrace{\prod_{s=2}^{T_\nu-1} \left[N_{T_u} \left(\{\beta_{gst}\}_{t=1}^{T_u}; \mathbf{0}, \sigma_{gs}^{-2} \Delta_2' \Delta_2 \right) \cdot p(\sigma_{gs}^2, \rho_g) \right]}_{\text{prior (2.7) and hyperpriors of the smoothing parameters}} \times \underbrace{p(\boldsymbol{\lambda})}_{\text{hyperprior for } \mathbf{Z}}, \tag{2.9}
 \end{aligned}$$

- **Goal:** Joint distribution $[\mathcal{P}, \mathbf{Z}]$ (data+unknowns) → Posterior distribution $[\mathbf{Z} | \mathcal{P}]$ (unknown given data)
- **Tool:** Markov chain Monte Carlo (MCMC)
- **Idea:** Simulate samples from the joint posterior distribution of the unknowns given the data;

Step I-C: Posterior Inference of the De-Warping

Joint distribution $[\mathcal{P}, \mathbf{Z}]$:

$$\begin{aligned}
 & \prod_{g=1}^G \underbrace{\left[\prod_{i=1}^{N_g} \left[\prod_{j=1}^{J_{gi}} N(T_{gij}; \mathbf{B}_{g1}(\nu_{Z_{gij}})'\boldsymbol{\beta}_g \mathbf{B}_{g2}(u_{gi}), \sigma_\epsilon^{-2}) \mathbf{1}\{T_{gij} \in \mathcal{I}_{gij}(\nu_{Z_{gij}}, A_0)\} \right] \right]}_{\text{likelihood (2.2)}} \\
 & \times J_{gi}! \underbrace{\left[\prod_{j=1}^{J_{gi}} \text{Categorical}(Z_{gij}; \boldsymbol{\lambda}) \mathbf{1}\{Z_{gij} \leq Z_{gi,j+1}, j = 1, \dots, J_{gi} - 1\} \right]}_{\text{prior of } \mathbf{Z}} \\
 & \times \underbrace{N_{T_\nu-1} \left(\{\beta_{gs1}\}_{s=1}^{T_\nu-1}; \boldsymbol{\beta}_{[-T_\nu]}^{\text{id}}, \sigma_{g1}^{-2} \Delta_1' \Delta_1 \right) \mathbf{1}\{\nu_0 = \beta_{g11} < \dots < \beta_{gs1} < \dots < \beta_{g,T_\nu-1,1} < \nu_{L+1}\} \cdot p(\sigma_{g1}^2)}_{\text{prior (2.6) and hyperprior of the smoothing parameter}} \\
 & \times \underbrace{\prod_{s=2}^{T_\nu-1} \left[N_{T_u} \left(\{\beta_{gst}\}_{t=1}^{T_u}; \mathbf{0}, \sigma_{gs}^{-2} \Delta_2' \Delta_2 \right) \cdot p(\sigma_{gs}^2, \rho_g) \right] \}_{s=2}^{T_\nu-1} \times \underbrace{p(\boldsymbol{\lambda})}_{\text{hyperprior for } \mathbf{Z}}, \tag{2.9}
 \end{aligned}$$

prior (2.7) and hyperpriors of the smoothing parameters

- **Goal:** Joint distribution $[\mathcal{P}, \mathbf{Z}]$ (data+unknowns) → Posterior distribution $[\mathbf{Z} | \mathcal{P}]$ (unknown given data)
- **Tool:** Markov chain Monte Carlo (MCMC)
- **Idea:** Simulate samples from the joint posterior distribution of the unknowns given the data; Then use the samples to do posterior inference for any functions of the unknowns

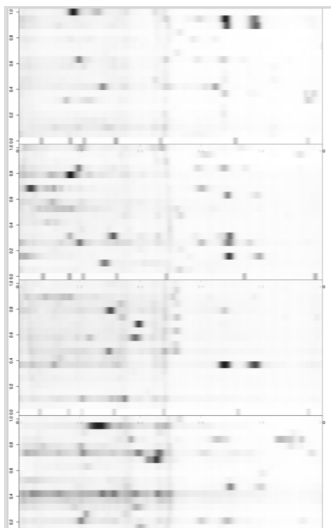
Step I-C: Align the peaks – Result

Animation; “ Δ ” for signature; “ \bullet ” for the observed peaks

(Please [Click the Image](#) for Animation)

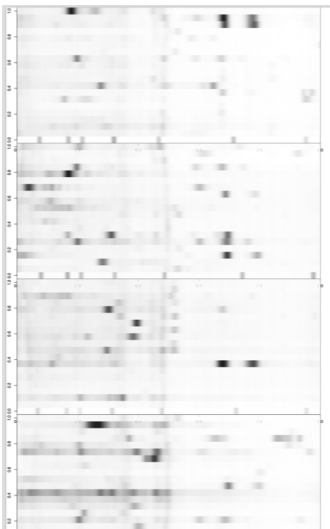
Step I-C: Aligned High-Frequency Intensity Data

Before



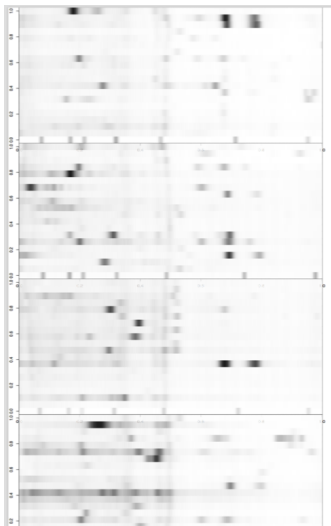
Step I-C: Aligned High-Frequency Intensity Data

Before

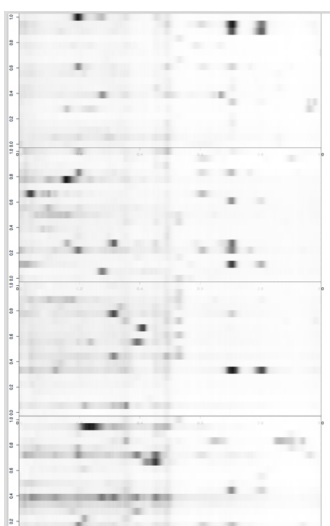


Step I-C: Aligned High-Frequency Intensity Data

Before

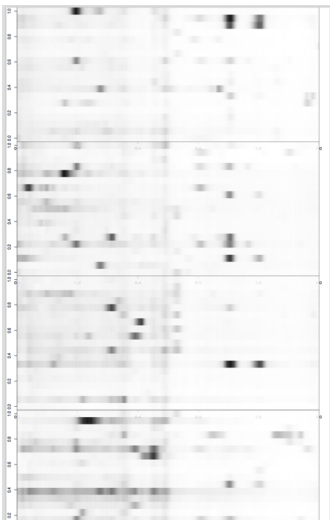
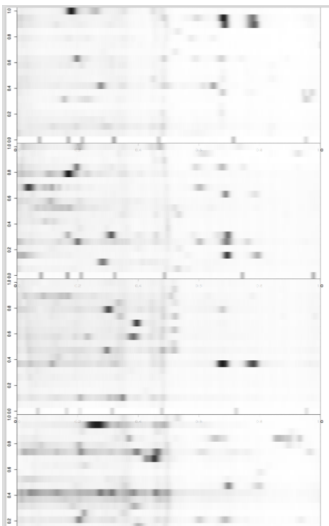


After



Step I-C: Aligned High-Frequency Intensity Data

Before note the curvatures are removed → After



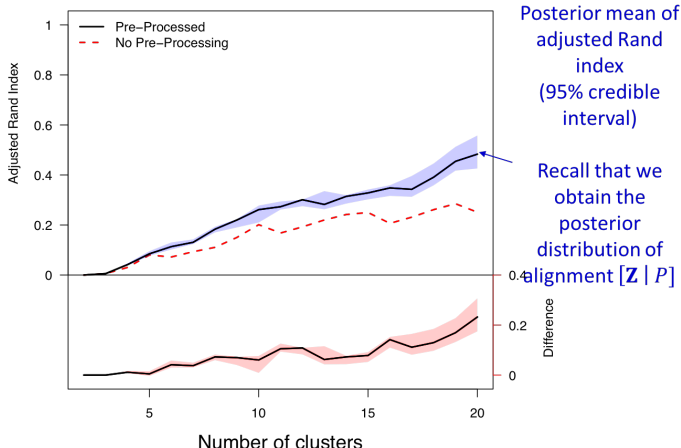
Data

Scleroderma

- Long-term clinical objective: find autoantibody signature that subsets autoimmune disease patients into groups with more homogeneous phenotypes and trajectories
- Sera from well-characterized patients with scleroderma and an associated cancer from Johns Hopkins Scleroderma Center database
- Data
 1. Known clustering: two replicate GEA experiments on 20 samples
 2. Unknown clustering: non-replicate GEA experiment on 80 samples
- Steps:
 1. Pre-processing
 2. Clustering (into 2, 3, ..., N groups) based on the pre-processed high-frequency intensity data (hierarchical clustering here)
 3. Evaluate the separation of the obtained clusters and compare them to the truth (known in the replicate experiment)

Pre-processing Improves the Accuracy of Cluster Estimation

Data with **technical replicates**; 20 samples, long- and short- exposures

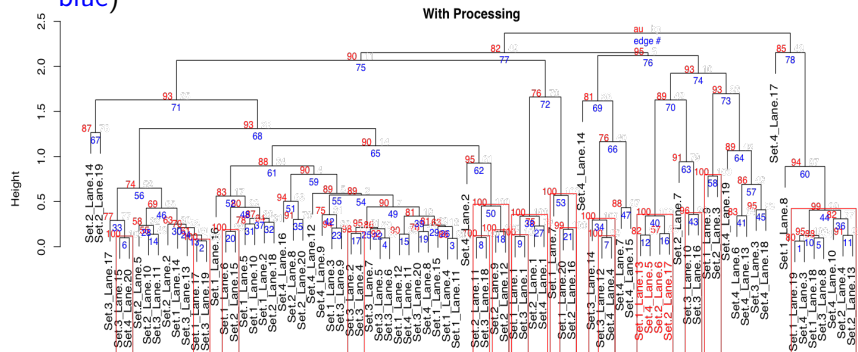


* Adjusted Rand index: assess the similarity of two ways of clustering the same set of observations; the higher the better

Pre-processing Improves the Separation of Clusters

Data without Replicates; Hierarchical Clustering; Pre-processed vs Non-Pre-processed

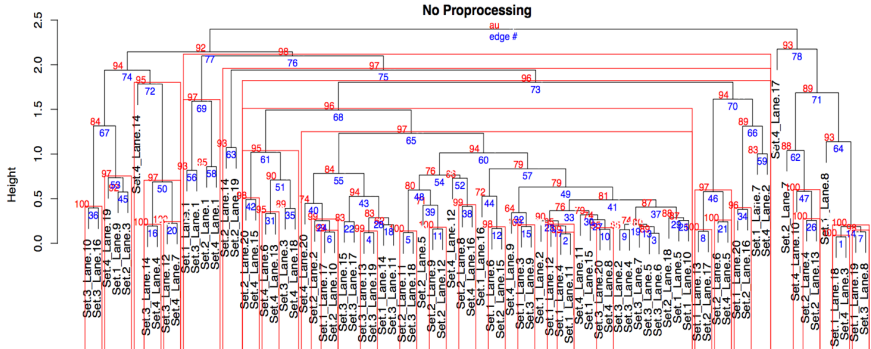
- **Distance**: Correlation-based distance; complete linkage
 - **Interpretation**: adjacent terminal nodes in the tree → similar in AutoAntibody signatures
 - **Uncertainty**: confidence levels by multiscale bootstrapping (**red** numbers; ones > 95 are shown in **red** boxes; a numbering of the subtrees is shown in **blue**)



Pre-processing Improves the Separation of Clusters

Data without Replicates; Hierarchical Clustering; Pre-processed vs Non-Pre-processed

- **Distance**: Correlation-based distance; complete linkage
 - **Interpretation**: adjacent terminal nodes in the tree → similar in AutoAntibody signatures
 - **Uncertainty**: confidence levels by multiscale bootstrapping (**red** numbers; ones > 95 are shown in **red** boxes; a numbering of the subtrees is shown in **blue**)



Summary

- **Problem:** Human recognition of autoantibody patterns and hence clustering becomes more difficult when patterns are composite and on multiple gels
- **Method:** Novel automated algorithms that
 1. Estimate autoantibody signatures
 2. The pre-processed data (Step I) can be the input of many **subgroup discovery** methods (Step II) including hierarchical clustering, latent class models and factor analyses
 3. Improves the accuracy of subgroup discovery
- Free publicly available open-source **software**:
<https://github.com/zhenkewu/spotgear>
- **Manuscript:** Wu, Casciola-Rosen, Shah, Rosen, Zeger (2017).
<http://biorxiv.org/content/early/2017/04/21/128199>
- **Ongoing work:** novel Bayesian clustering model to find disease subsets; Based on the biology that autoantibodies recognize protein complexes.

Thank You!

Funding

Patient-Centered Outcome Research Institute [PCORI ME-1408-20318]
Hopkins Individualized Health Initiative

Some References (More at: zhenkewu.com)

- **Wu Z, Casciola-Rosen L, Shah AA, Rosen A, Zeger SL (2017+).**
Estimating AutoAntibody Signatures to Detect Autoimmune Disease Patient Subsets.
Minor Revision for *Biostatistics*. <http://biorxiv.org/content/early/2017/04/18/128199>.
- **Wu Z, Deloria-Knoll M, Hammitt LL, and Zeger SL, for the PERCH Core Team (2015).**
Partially Latent Class Models (pLCM) for Case-Control Studies of Childhood Pneumonia Etiology.
Journal of the Royal Statistical Society: Series C (Applied Statistics). 65:97-114.
- **Wu Z, Deloria-Knoll M and Zeger SL (2016a).**
Nested Partially-Latent Class Models for Estimating Disease Etiology from Case-Control Data.
Biostatistics, 18 (2): 200-213. doi:10.1093/biostatistics/kxw037.